

Modelling the suitability of EMCCDs for spectroscopic applications

Simon Tulloch

Isaac Newton Group of Telescopes, Apartado 321, Santa Cruz de La Palma,
Islas Canarias, 38700, SPAIN

ABSTRACT

A model of EMCCDs has been developed to predict the areas of application where they offer superior performance to a conventional CCD. The sub electron read noise of an EMCCD makes it an obvious choice for observations that are normally detector noise limited, for example the detection of faint emission lines. In other regimes where photon noise is dominant, for example the measurement of absorption lines or emission lines superimposed on a bright continuum, EMCCDs offer less advantage. This model is used to generate a large number of synthetic spectral lines both in absorption and emission, including the effects of clock induced charge and multiplication noise. The line parameters are then measured by fitting a Gaussian profile and the 'goodness of fit' of this profile used to calculate the SNR of the measurement. The model allows the performance parameters of the EMCCD to be varied freely to see the effect on SNR. As a confidence check, the model is compared against actual images taken with an EMCCD camera in the laboratory.

Keywords: EMCCD L3 CCD ING CV Noise Modelling

1. INTRODUCTION

1.1 EMCCD characteristics

Electron Multiplying CCDs (EMCCDs) use charge domain signal amplification, using an avalanche multiplication register, to overcome the limitations of output-amplifier induced read noise. In the read noise dominated regime, which is generally speaking where the signal level per pixel is less than the square of the read noise, an EMCCD can deliver a considerable boost to the SNR. The avalanche gain is in fact so high; several thousand is easily achieved, that the amplifier read noise becomes insignificant. This gives a new flexibility in the operation of the CCD. In the particular case of spectroscopy it means that the detector resolution, both temporal, spatial and spectral can be decided *after* the observations are completed. For example, if we wish to do high time resolution observations of a new source that we know to exhibit short period changes then we can set the frame rate fairly high to cover all eventualities. Post readout temporal binning can then be applied, *with almost no noise penalty*, to match the effective frame rate to the rate of change of the object. With a conventional CCD we are much more restricted and we have to decide on an optimum frame rate prior to observing; any post readout binning will introduce additional noise. The same principle applies to our choice of spectral and spatial resolution. If for example we wish to measure the radial velocity of a star in a short period double system then with a conventional CCD we need to decide in advance what grating dispersion we should use to get the required velocity resolution without spreading the light too thinly across the detector. With the EMCCD we have the flexibility to use a high dispersion grating to cover all eventualities and then later binning down to the optimum resolution. Additionally, the read noise of the EMCCD remains negligible independently of pixel rate which opens up new possibilities for high speed spectroscopy and photometry.

The avalanche multiplication architecture on the EMCCD uses a gain register containing several hundred stages each having a fairly low gain. An unavoidable consequence of this is that a single electron entering the register can give rise to a whole spread of output values. This constitutes an additional noise known as Multiplication Noise. The effect is to increase the Poissonian noise in the signal by a factor of 1.4. The effect on the SNR is identical to that of a halving of detector QE. The multiplication noise starts to dominate at higher signal levels so there comes a point where a conventional CCD delivers a superior SNR to an EMCCD. This point occurs, if we choose to consider the SNR on a pixel by pixel basis with no on-chip binning, when the signal is approximately equal to the square of the read noise of the conventional CCD. Since the astronomical objects we observe typically cover many pixels the actual situation is somewhat different and the EMCCD is superior up to much higher signal levels than might be supposed from a single pixel noise analysis.

Whilst free of read noise, EMCCDs do suffer from a further noise source that limits their operation for very low illuminations. This is Clock Induced Charge or CIC. This takes the form of stray electrons randomly distributed in the image, generated by the CCD clocks during the readout process. Individually they are indistinguishable from photo-electrons and so constitute a faint background. In the case of the EMCCD camera in use at the Isaac Newton Group, the CIC is roughly equivalent to the signal from a dark sky using 15s exposures with the R1200 grating on the ISIS instrument.

Almost all commercially available EMCCDs are of Frame Transfer (FT) architecture. This means that they can be read out whilst a subsequent exposure is under way. If high frame rates are used this can give a large observational advantage. FT architecture can of course be applied to a conventional CCD although it is not generally done for larger science devices which are almost always used with mechanical shutters. This is not so surprising given that an FT CCD requires up to twice the silicon area of a mechanically shuttered one and high frame rates are only needed in a few specialised regimes.

The EMCCDs manufactured by E2V (known as 'L3CCDs') contain two selectable outputs, the second of which has a conventional low noise (approx $3.3e^-$) amplifier. The user has the freedom to choose which output is best for a given application.

1.2 EMCCD observations at the William Herschel Telescope (WHT)

The WHT has two EMCCDs available. The first is in a wavefront sensor camera used in conjunction with a laser based AO system. The second, QUCAM2, is a general purpose cryogenic 1K x 1K pixel camera used with the ISIS instrument for high frame rate spectroscopy. This camera has both an EMCCD output and a conventional output which are selectable from the observing interface. It has been used to observe Cataclysmic Variable stars (CVs). This class of object consists of a White Dwarf primary accreting material from a lower mass companion in a close orbit. Orbital periods range from 5 minutes to over a day and many new members discovered by the SDSS survey are fainter than magnitude 18. Observations of these objects with a conventional CCD would be wholly swamped by detector read noise.

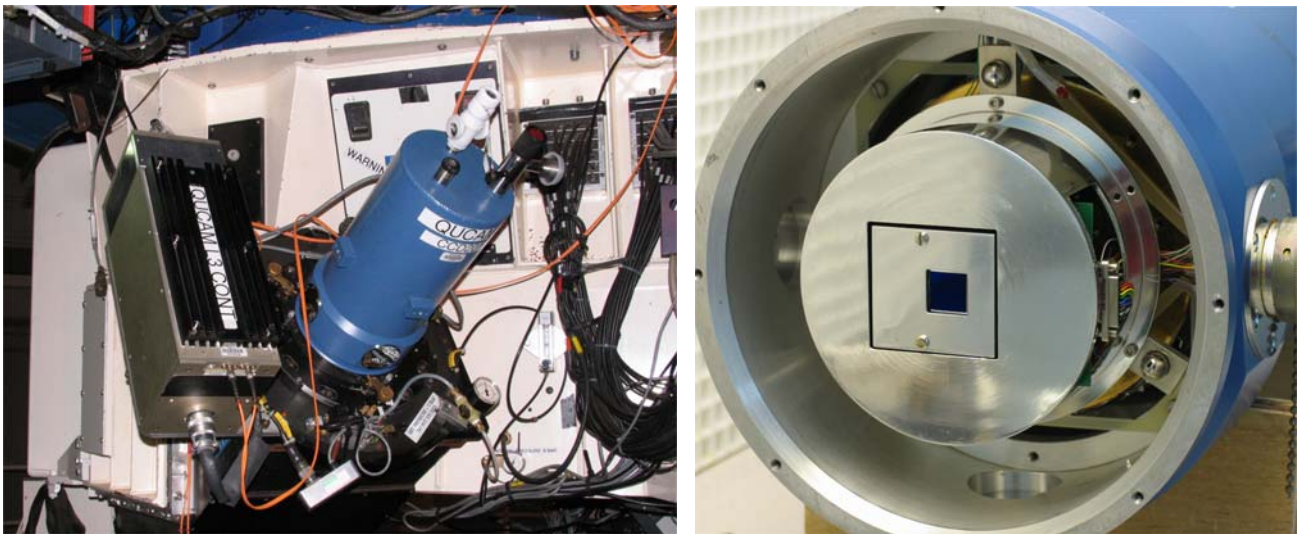


Fig. 1. EMCCD mounted on the ISIS spectrograph of the WHT. Internal view of camera cryostat also shown.

1.3 The need for a model of an EMCCD

The advantage of the EMCCD output of our camera for CV observations is quite clear cut since the faint spectral lines we observe have a peak intensity of 5 to 10 photo-electrons per 30s exposure. Observers at the WHT wishing to make other types of observations need to know up to what point the EMCCD output remains competitive and at which point they should swap to the conventional output or perhaps consider a more conventional camera. With this in mind an EMCCD model was developed that could be used to predict the SNR of spectrographic observations in various observational regimes.

2. THE EMCCD MODEL

The model is written in IDL and runs on a typical windows PC where it is able to generate and analyse about 90 spectra per second, each measuring 200 x 32 pixels. Two such spectra, consisting of a single emission line superimposed upon a continuum and an absorption line are shown below. Note the faint peppering of CIC in the background.

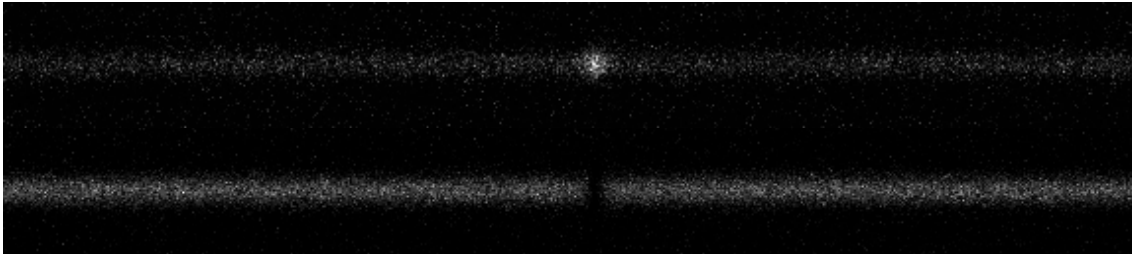


Fig.2. Synthetic emission and absorption spectra generated by the EMCCD model.

2.1 Parameters included in the model

The model allows the following parameters to be adjusted:

- clock induced charge
- read noise of output amplifier
- EMCCD gain factor
- Amplitude of spectral line (both +ve and -ve)
- Dark current
- On chip spatial binning factor
- observational efficiency (shutter losses)
- FWHM of spectral line in spatial direction
- FWHM of spectral line in spectral direction
- Level of continuum
- Sky background
- Off chip spatial binning factor

With this flexibility of parameters, the model can in fact simulate any CCD both conventional and electron multiplying. Comparisons of EMCCD and conventional CCDs are then possible for varying signal levels (both line amplitude and continuum level), line widths, seeing conditions, binning factors and sky background levels. For the purpose of this study some of the parameters remained fixed to typical operational values. These are listed below together with their values:

clock induced charge from image area: $0.02e^-$ per pixel per readout
clock induced charge from gain register: $0.01e^-$ per pixel per readout (image area equivalent electrons)
read noise , conventional CCD: $3.3e^-$
read noise , EMCCD: $20e^-$
EMCCD gain factor: 196
dark current: 0
sky background: 0
observational efficiency: 1 (no shutter losses since we have FT architecture)
spatial scale: 5.2 pixels per arcsecond
seeing: 1"
On-Chip spatial binning factor :2
Off-Chip spatial binning factor:3 (so as to include full spatial extent of spectrum in 1 row)

Note: The product of the two binning factors is the effective width of the extraction window

The remaining parameters : line strength and width and the continuum strength were varied freely.

2.2 Principle of operation of the model

The first part of the model generated the synthetic spectra based on the input parameters listed above. The spectra were then reduced to one dimension through off-chip binning and transferred to a Gaussian fitting routine (actually the standard IDL 'GAUSSFIT' procedure) to yield their key values of line height, line width, line centre and constant (or continuum) term. By generating sets of several thousand spectra and then measuring the RMS variation of these basic measured values, we can see how measurement noise is affected by our input parameters. At very low line amplitudes the Gaussian fitting routine would often fail to do a proper fit and it was important to filter out these mis-fits so as not to disturb the end result. This was done by comparing the measured line width with the actual known line width. Large discrepancies resulted in that spectrum being excluded from the subsequent statistical analysis. Lines with peak amplitudes below $10e^-$ were not considered at all since they contained insufficient information for the Gaussian fitting routine to converge on a result.

A typical run of the model consists of deciding first on the continuum level and width of the spectral line and then running through various spectral line amplitudes ranging from $-1 \times$ continuum up to approximately $700e^-$. At each amplitude step, 1000 images are generated using the EMCCD amplifier characteristics, 1000 more using the conventional output and a further 1000 using the conventional amplifier but including the effects of a 2 fold on-chip spatial bin. Further runs were then done for different continuum and line width values. With so many potential variables it is easy to become swamped by the results and so it was necessary to focus on those variables that most strongly affect the competitiveness of the EMCCD and fix others to their typical observational values.

2.3 Noise models for conventional and EMCCDs

The noise model used by the Gaussian fitting program is of crucial importance. It describes the uncertainty to which each wavelength step value in the extracted 1D spectrum is known. Without an accurate noise model the fitting program will not give sensible results. The noise model for the conventional CCD is the following standard equation (1) where the photon noise and amplifier read noise N , are added in quadrature.

$$Errors_{NORM} = \sqrt{(Signal + N^2 \cdot LBin_{OFF} \cdot SBin_{OFF})} \quad 1)$$

It has the small additional term to account for the off chip spatial binning factor $SBin_{OFF}$, required to reduce the spectrum to 1D for analysis. In the case of the EMCCD the noise model must also account for the multiplication noise and the fact that the amplifier noise is effectively divided by the numerical gain of the multiplication register G_{EMCCD} .

$$Errors_{EMCCD} = \sqrt{(2 \times Signal + (N / G_{EMCCD})^2 \cdot LBin_{OFF} \cdot SBin_{OFF})} \quad 2)$$

In the two equations above, *Signal* actually refers to the number of electrons present in a wavelength step of the extracted spectrum (i.e. the end product of the CCD observation). Some of this signal will be contributed by other sources than the spectral line, as defined below (3) for a system with the spectral axis lying along a CCD image row:

$$\begin{aligned} Signal = & \\ & CIC_S \cdot SBin_{OFF} \cdot LBin_{OFF} \\ & + (CIC_P + S + D) \cdot SBin_{ON} \cdot SBin_{OFF} \cdot LBin_{OFF} \cdot LBin_{ON} \\ & + CONTINUUM + LINE \end{aligned} \quad 3)$$

Where:

CIC_S = clock induced charge originating in the multiplication register

CIC_P = clock induced charge originating in the image and store area

$SBin_{ON}$ = on-chip spatial binning factor

$SBin_{OFF}$ = off-chip spatial binning factor

$LBin_{ON}$ = on-chip spectral binning factor
 $LBin_{OFF}$ = off-chip spectral binning factor
 S = photoelectrons per pixel per frame from sky background
 D = photoelectrons per pixel per frame from dark current
 $CONTINUUM$ = photoelectrons per pixel wavelength step per frame from the continuum
 $LINE$ = photoelectrons per pixel wavelength step per frame from the spectral line

Notes: the last two parameters are expressed 'per wavelength step' whereas the others are 'per pixel'. The CIC originating in the multiplication register, CIC_S , is that measured in the serial over-scan of the image. The image area contains both CIC_S and CIC_P . These two components are measured from the sum of many bias frames.

The main purpose of this study is to show how the noise in the measurement of Gaussian profile spectral line parameters varies with the line and the detector characteristics, however, it is also interesting to see how the SNR within a single wavelength step of the *final 1D extracted spectrum* responds to these variations. The above noise model equations can be used to do this. The observational parameters are quoted in section 2.1. although various values for the off-chip spatial binning are used for the conventional CCD since this has a significant effect on its performance. For a conventional CCD, off-chip binning is not a noiseless process whereas for the EMCCD it *is* almost noiseless.

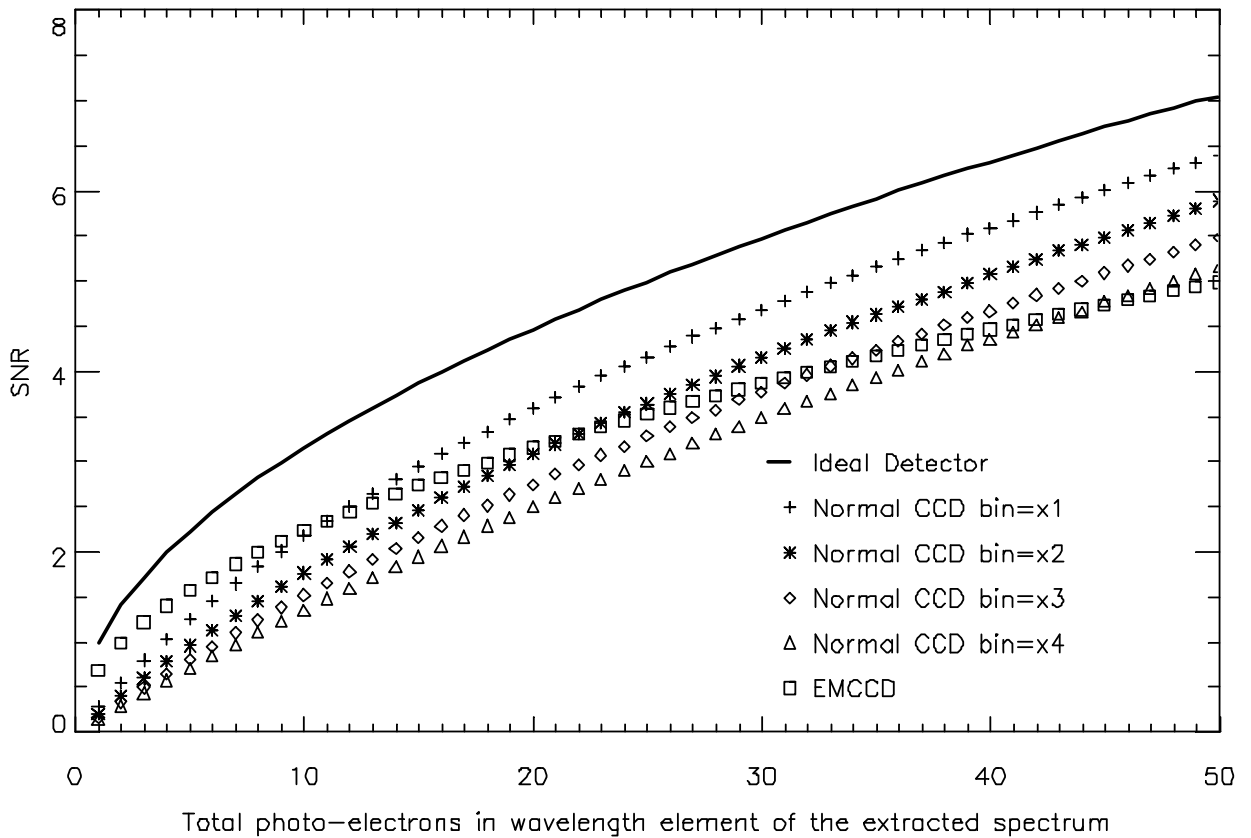


Fig.3. SNR within a single wavelength element of the final extracted spectrum. A comparison of an EMCCD and a Normal CCD with various degrees of off-chip binning. Note how the EMCCD becomes progressively less competitive at higher signal levels due to the effects of multiplication noise.

The graph shows that the position of the cross over point depends greatly on the off-chip binning factor used with the conventional detector. With typical ISIS spatial binning factors (x2 or x3) the EMCCD loses its competitiveness, when analysed on a pixel by pixel basis, at signal levels of between 20 and 30e⁻ in the extracted spectrum.

3. LAB BASED CONFIRMATION OF THE MODEL

With such a complex model there is clearly ample opportunity for errors to creep in and indeed considerable effort was spent in the debugging phase. A lab based confirmation of the model's accuracy was therefore essential.

3.1 Generation of Emission line images in the laboratory

Our EMCCD camera was fitted with a standard camera lens and mounted in a dark room. It was focussed up on a faintly illuminated pinhole and left to settle for several hours. Blocks of 500 images were then taken of the pinhole at various exposure levels and through both outputs of the camera. A single high SNR exposure taken through the conventional output was analysed to give the actual spot parameters of brightness and FWHM in both axes and also to confirm that dark current and stray light were at negligible levels. A bias was also taken to measure the read noise. No on-chip binning was done. The conventional output was used for these measurements owing to its superior gain stability. The spot images were thus accurate representations of emission line spectra with a zero continuum, but required none of the complications of setting up a spectrograph in the laboratory.

3.2 Model predictions versus the real data

There was good agreement between the model and the lab based measurements. The graphs below show the comparison.

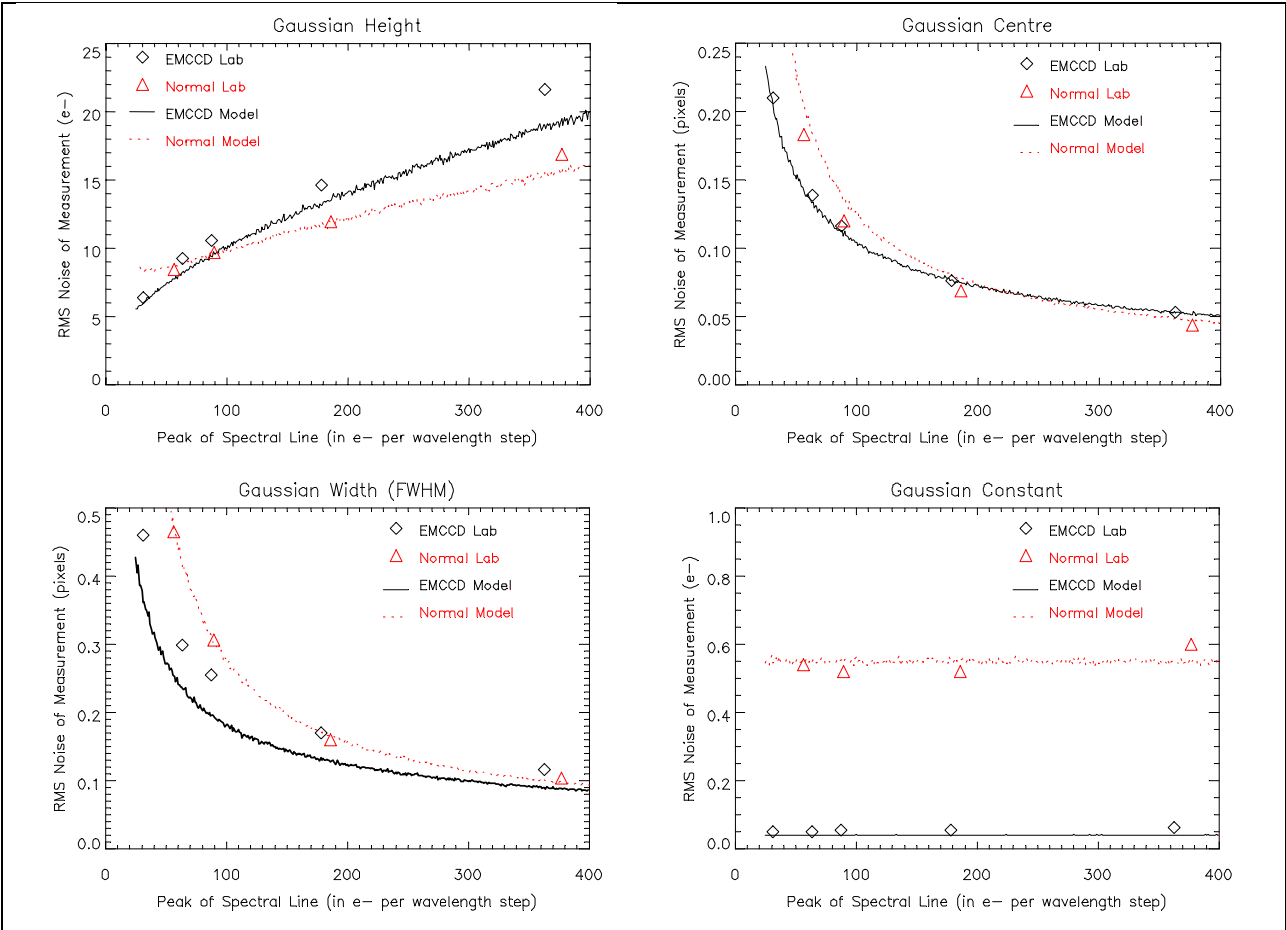


Fig.4. Comparison of real data with the predictions of the model. Line width was 2.84 pixels FWHM. Read noise was 3.3e⁻ No on-chip binning.

4. EXTRAPOLATION OF THE MODEL TO OTHER REGIMES

There are clearly many variables that we can vary in order to compare the relative advantages of normal and EMCCDs. The single pixel analysis that is shown in section 2.3, experiments with variations in the binning factor demanded by differing levels of seeing. There are other important variables whose effect can only be investigated if we consider the image of a spectral line as a whole. For example, when analysing a spectral line how are the accuracy of its parameters affected by the width of the line and the level of the underlying continuum? It would seem reasonable to assume that a broad line whose photons are spread thinly across the CCD will be measured more accurately with an EMCCD. It would also seem reasonable to assume that a bright continuum will favour the use of a conventional CCD since the Poissonian noise in the continuum will mask the contribution of detector read noise. The relative pros and cons of the two CCD types for measuring absorption lines are more difficult to predict. The Model was used to investigate all these variables

4.1 EMCCD performance: Emission lines with no continuum

The Model was used to generate and measure emission line spectra with FWHMs of both 5 and 50 pixels and with the continuum set to zero. Section 2.1. quotes the other image and camera characteristics. Depending on which Gaussian parameter we are interested in measuring, the EMCCD is competitive up to surprisingly high signal levels.

Table 1 : Emission Lines with no continuum

Gaussian Parameter	Peak brightness (e^-) of extracted Line for EMCCD still to be competitive	
	Line FWHM=5 Pixels	Line FWHM=50 Pixels
Height	55	75
Centre	140	140
Width	400	700
Constant	EMCCD always better	EMCCD always better

4.2 EMCCD performance: Emission and Absorption lines superimposed upon a continuum.

Again, narrow and broad spectral lines were modelled but this time with varying levels of underlying continuum, ranging from $10e^-$ to $100e^-$ per pixel of the extracted spectra. With the higher levels of continuum it was also possible to model lines with negative amplitude i.e. absorption lines. Note that the peak brightness of the spectra quoted below refers to the height of the line once the continuum has been subtracted.

Table 2 : Emission Lines with continuum $=10e^-$ per pixel in the extracted spectra.

Gaussian Parameter	Peak brightness (e^-) of extracted Line for EMCCD still to be competitive	
	Line FWHM= 5Pixels	Line FWHM=50 Pixels
Height	35	40
Centre	70	65
Width	130	170
Constant	EMCCD always better	EMCCD always better

Table 3 : Emission Lines with continuum $=30e^-$ per pixel in the extracted spectra.

Gaussian Parameter	Peak brightness (e^-) of extracted Line for EMCCD still to be competitive	
	Line FWHM=5 Pixels	Line FWHM=50 Pixels
Height	5	10
Centre	20	10
Width	20	25
Constant	EMCCD always better	Same at all signals

Table 4 : Emission Lines with continuum =100e⁻ per pixel in the extracted spectra.

Gaussian Parameter	Peak brightness (e ⁻) of extracted Line for EMCCD still to be competitive	
	Line FWHM=5Pixels	Line FWHM=50Pixels
Height	-65	-80
Centre	EMCCD always worse	EMCCD always worse
Width	EMCCD always worse	EMCCD always worse
Constant	EMCCD always worse	EMCCD always worse

There is insufficient space here to show the full graphical output of the model. Fig 5. shows the particular case of the continuum equal to 100e⁻ for a spectral line of FWHM=5pixels. This figure shows how the SNR of the measured Gaussian parameters varied as the spectral line changes from being a saturated absorption line up to being an emission line with a peak of 200e⁻ (above continuum). Note how the EMCCD generally gives a worse performance, except in its measurement of the depth of very deep absorption lines. Clearly for such high continuum levels the conventional CCD should be chosen.

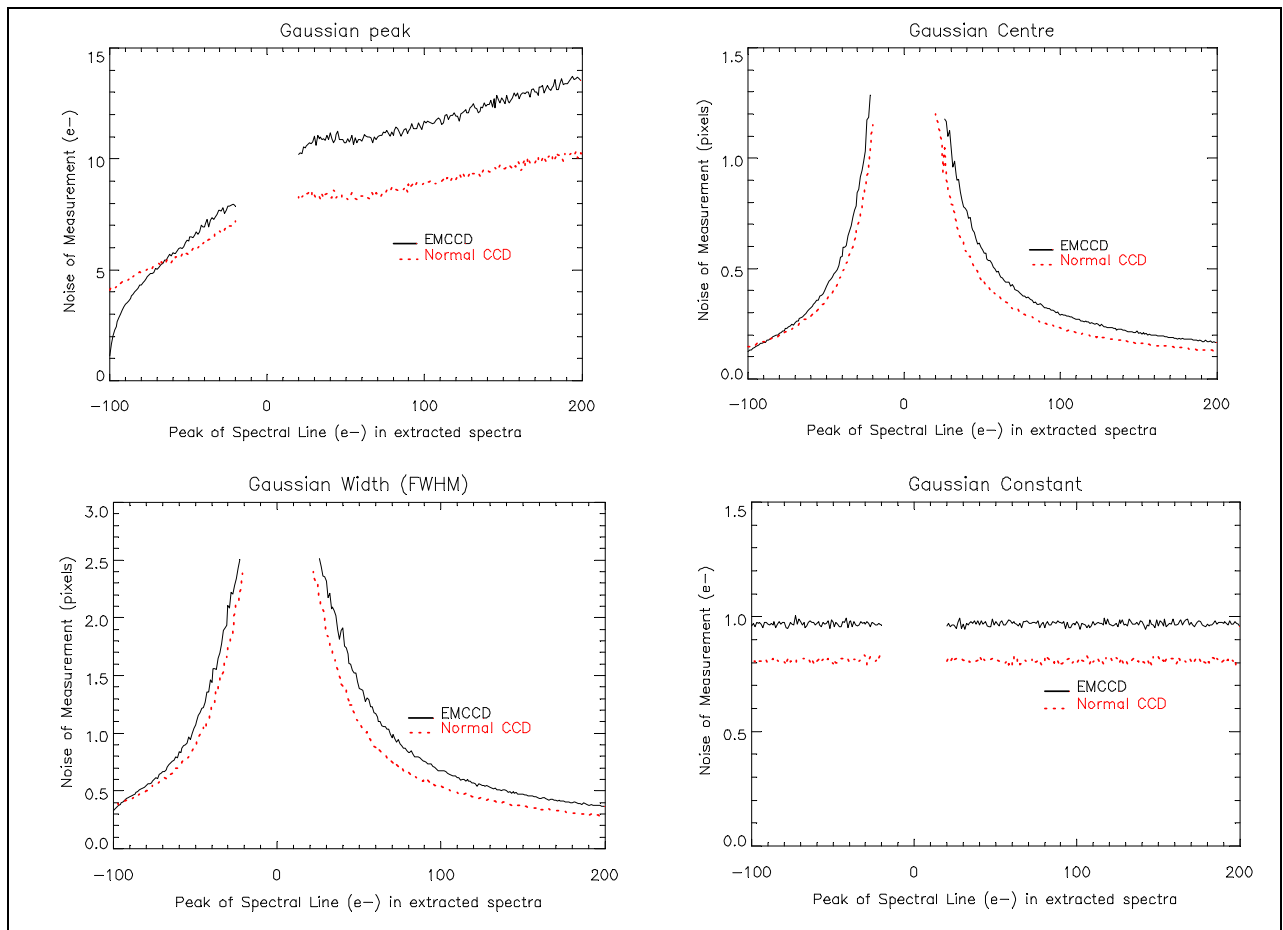


Fig.5. Continuum 100e⁻, line width=5 pixels FWHM. On-chip spatial binning was x2 , off-chip x3

5. QUALITATIVE LABORATORY COMPARISON

A further qualitative comparison was made using a USAF test target alternatively illuminated from the front and from behind. This demonstrated quite nicely how the relative advantage of the EMCCD output rapidly disappears as the exposure level increases. Fig 6) shows the rear illuminated situation which approximates to the case of emission lines with a zero continuum. Each image shows the conventional output on the left with the EMCCD output to the right. The images are mirrored with respect to each other, a consequence of the amplifiers being situated at opposite ends of the horizontal register of the CCD. Even with a peak exposure of $2.2e^-$ per pixel the test target is just visible from the EMCCD output. At about $6e^-$ per pixel exposure it becomes visible in the conventional output. At $22e^-$ per pixel exposure the two outputs give about the same level of detail.

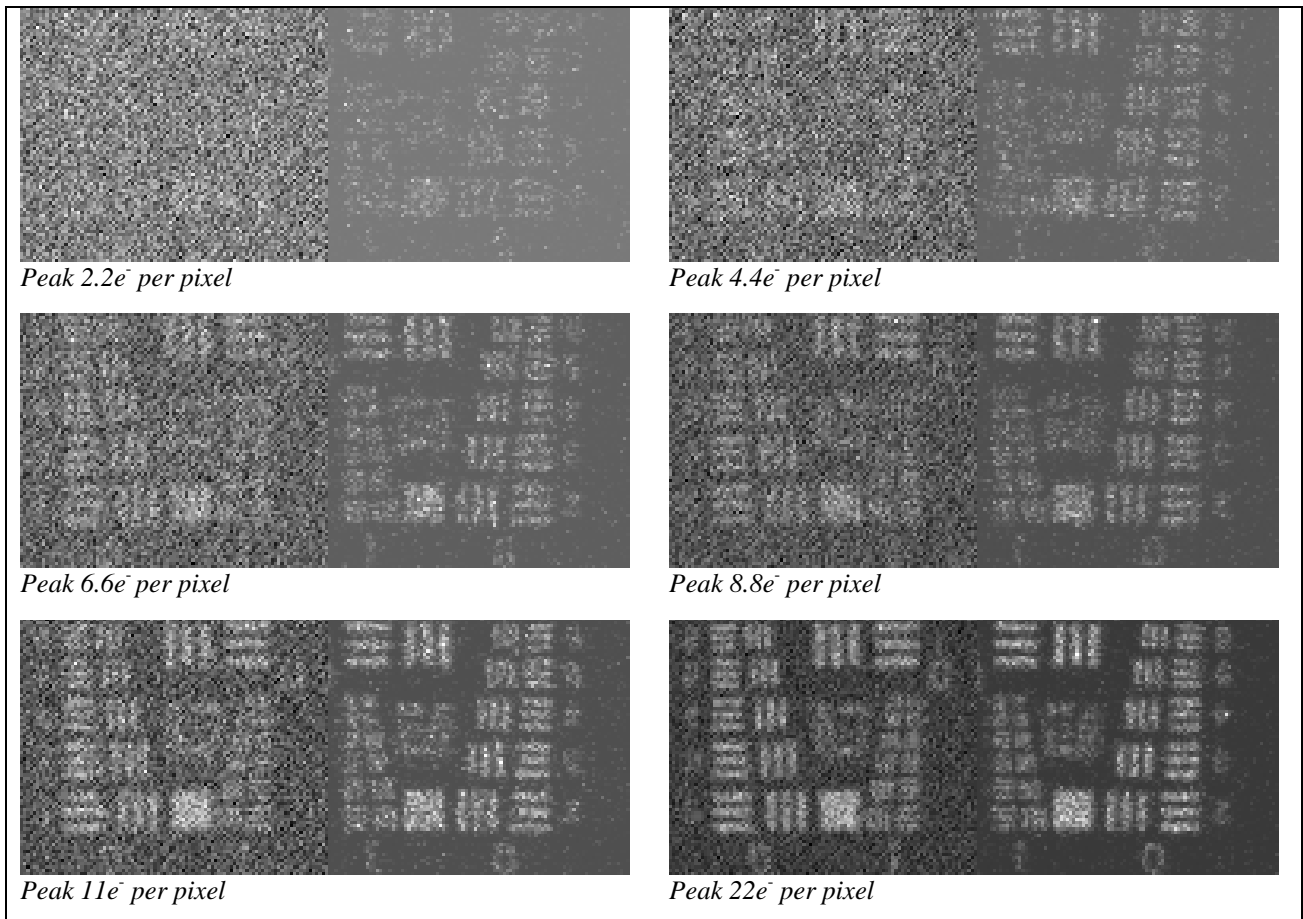


Fig 6. Conventional (left) versus EMCCD (right) test patterns compared. Test Pattern in Emission. No binning. Read noise= $3.3e^-$

The test target was then placed in front of a black background and illuminated from the front thus producing a negative test pattern. This situation approximates to the case of deep absorption lines. The resultant images are shown in Fig. 7. Notice that the EMCCD only gives an advantage at extremely low illumination levels; once the exposure reaches $10e^-$ per pixel, its advantage has disappeared.

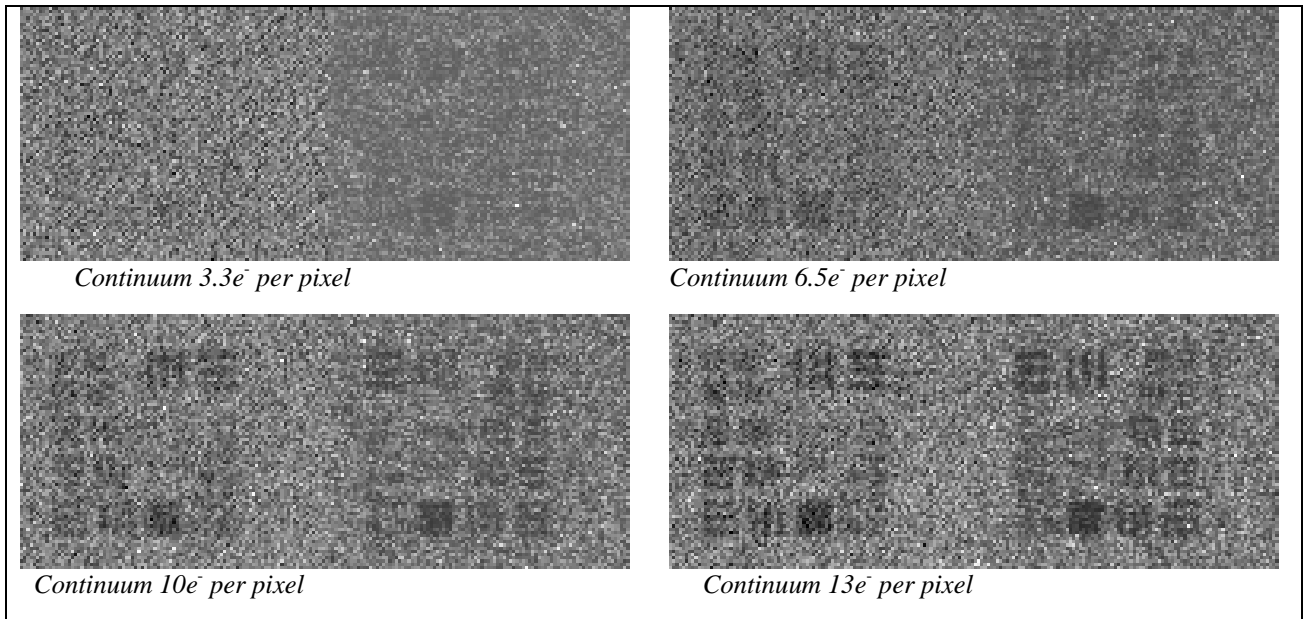


Fig 7. Conventional (left) versus EMCCD (right) test patterns compared. Test Pattern in Absorption. No binning. Read noise= $3.3e^-$

6. CONCLUSIONS

When considering the relative merits of the two CCD types it was important to analyse their performance based upon the statistics of the final extracted spectrum. Any off chip binning had almost no effect on the SNR of the EMCCD whilst it made a huge difference to that of the conventional detector. Using a x2 on chip spatial bin followed by a x3 off-chip spatial bin (typical values for ISIS with seeing= $1''$), we can conclude the following:

- 1) For zero continuum, EMCCD is always best up to peak line brightness up to $60e^-$.
- 2) Once the continuum is at $10e^-$ the EMCCD advantage is already severely reduced
- 3) With the continuum greater than $30e^-$ the EMCCD is only favoured for deep lines that approach saturation.
- 4) The relative merits of two CCD types only weakly affected by the spectral line width

The system sensitivity of the QUCAM2 camera on the WHT is $195 \text{ ADU}/e^-$ when using its EMCCD output. We are thus able to recommend a maximum exposure level, in the extracted spectra, above which the observer will get superior performance by switching to the conventional output of the camera. For the case of typical seeing conditions of $1''$ and an on-chip spatial binning factor of 2, this maximum exposure level will be around 12000 ADU. If the continuum exceeds about 1000 ADU we also recommend switching to the conventional output.